Journal of Saudi Chemical Society (2014) **18**, 802–813

King Saud University

**Journal of Saudi Chemical Society**

www.ksu.edu.sa
www.sciencedirect.com

ORIGINAL ARTICLE

# Adsorption of some metal complexes derived from acetyl acetone on activated carbon and purolite S-930

**Salam A.H. Al-Ameri** *, **Mahmoud N.A. Al-Jibouri, Taghreed M.D. Musa**

*Chemistry Department, College of Science, Al-Mustansiriyah University, Iraq*

Received 23 May 2011; accepted 22 September 2011
Available online 2 October 2011

**KEYWORDS**

Adsorption;
Isotherm;
Metal complexes;
Activated carbon;
Purolite S-930

**Abstract** A new Schiff base (HL) derived from condensation of *p*-anisidine and acetyl acetone has been prepared and used as a chelating ligand to prepare Cr(III), Mn(II), Co(II), Ni(II) and Cu(II) complexes. The study of the nature of these complexes formed in ethanol solution following the mole ratio method (2:1, L:M) gave results which were compared successfully with these obtained from isolated solid state studies. These studies revealed that the complexes having square planner geometry of the type ($ML_2$), M = Co(II), Ni(II) and Cu(II), and octahedral geometry of the type $[Cr^{III}L_2(H_2O)_2]Cl$ and $[MN^{II}L_2(H_2O)_2]$. The adsorption studies of three complexes Cr(III), Mn(II), and Co(II) on activated carbon, H and Na-forms of purolite S-930 resin show high adsorption percentage for Cr(III) on purolite S-930 due to ion exchange interaction compared with high adsorption of neutral Mn(II), Co(II) complexes on activated charcoal. Linear plot of log $Q_e$ versus log $C_e$ showed that the adsorption isotherm of these three complexes on activated carbon, H and Na-forms of purolite S-930 surface obeys Freundlich isotherm and was similar to S-curve type according to Giles classification which investigates heterogeneous adsorption. The regression values indicate that the adsorption data for these complexes fitted well within the Freundlich isothermal plots for the concentration studied. The accuracy and precision of the concentration measurements of these complexes were determined by preparing standard laboratory samples, the results show relative error ranging from ±1.08 to 5.31, ±1.04 to 4.82 and ±0.28 to 3.09 and the relative standard deviation did not exceed ±6.23, ±2.77 and ±4.38% for A1, A2 and A3 complexes, respectively.

## 1. Introduction

Metal complexes of Schiff base have played a central role in the development of coordination chemistry. From the survey of existing literature, it appears that acetyl acetone and its related complexes have been extensively used as biologically active (Sengupta et al., 1986), complexion agents, analytical

---

* Corresponding author. Mobile: +964 07702531868.
E-mail address: alamri_salam@yahoo.com (S.A.H. Al-Ameri).

Peer review under responsibility of King Saud University.

Production and hosting by Elsevier

http://dx.doi.org/10.1016/j.jscs.2011.09.012

agents (Zhu et al., 1990) and other industrial applications. The interactions between immobilized reagents and metal ions in solution have been widely investigated (Ramana and Sengupta, 1992). Metal impregnation of charcoal results in the modification of chemical properties, which allows utilization in various industrial applications. The linear form of Langmuir equation (1) is the most widely used two parameter equation commonly expressed as (Langmuir, 1918; Muthulakshmi and Sakthi, 2010; Vadi et al., 2010):

$$\frac{1}{Q_e} = \frac{1}{Q_m b C_e} + \frac{1}{Q_m} \tag{1}$$

where $C_e$ is the concentration of the metal complex remaining after adsorption (mg/L) and $Q_e$ is the amount of adsorbed metal complex per unit mass of resins at equilibrium (mg/g). $Q_m$ and $b$ are the Langmuir constants related to the adsorption capacity (mg/g) and energy of adsorption, respectively (Muthulakshmi and Sakthi, 2010). The value of $Q_m$ and $b$ are evaluated from the slope and intercept of the plot:

$$\frac{1}{Q_e} = V_s \frac{1}{C_e} \tag{2}$$

The Freundlich isotherm is an empirical equation which has been shown to satisfactorily describe adsorption at low concentration of solution (Freundlich, 1971). The equation is commonly given by:

$$Q_e = A C_e^{\frac{1}{n}} \tag{3}$$

where $A$ is a constant for the system, or represents the adsorption capacity related to the bonding energy.

The present study reports the synthesis, characterization, analysis and adsorption behavior of some metal complexes on activated charcoal and purolite S-930 ion-exchange resin.

## 2. Experimental

### 2.1. Materials and measurements

All reagents and solvents were of analytical grade obtained from commercial sources, Fluka (Bush, Switzerland), Riedel-de Haën (Seelze, Germany) and BDH and used as received without further purification. FT-IR spectra were measured and recorded as KBr and CsI disks in the range 4000–400 $cm^{-1}$ using FT-IR Tests cane Shimadzu model Spectrometer. UV–Vis spectra were recorded in ethanol and DMF using Shimadzu UV–Vis spectrophotometer with quartz cells of size 1 cm was used to determine the concentration of metal complexes by measuring the absorbance at $\lambda_{max}$ of each one ana-

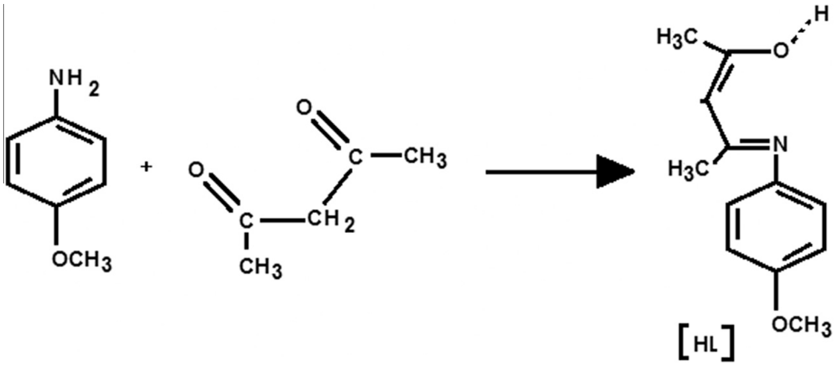

**Scheme 1** Synthesis of the (HL) ligand.

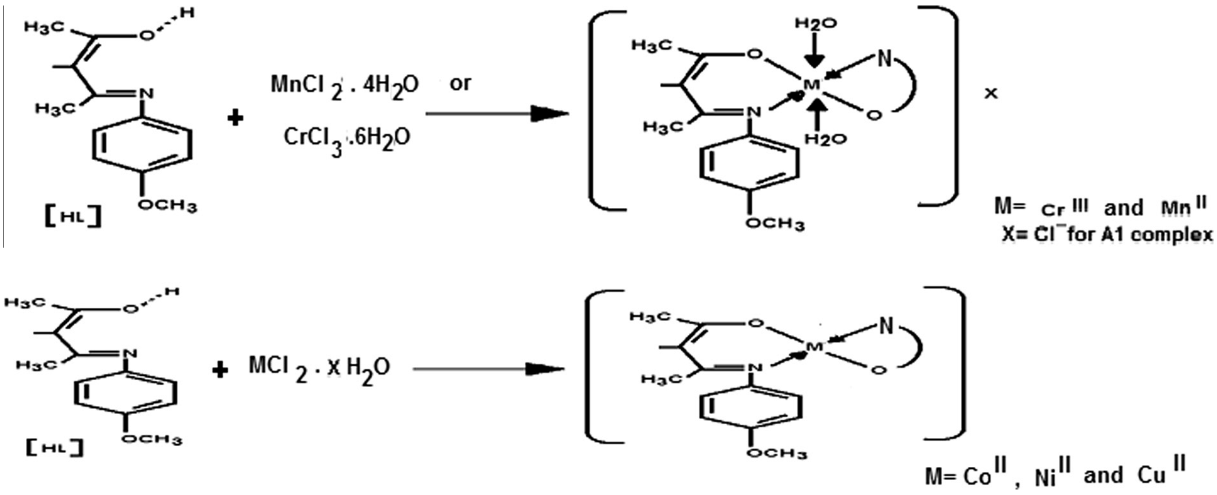

**Scheme 2** Synthesis of metal complexes.

lyte. Flame Atomic Absorption measurements were carried out using Shimadzu AA spectrophotometer. pH measurements were carried out using WTW pH-meter mode 720. Micro-analytical data were determined using Carlo-Erba-elemental analyzer in the King University, Jordon. Infers model shaker-incubator was used for solution stirring processes during equilibrium adsorption. Magnetic susceptibility measurements of the solid complexes were determined by a Gouy balance at 30 °C using mercury (II) tetrathiocyanate, Cobaltate(II) as a calibrant. Molar conductivity measurements were made with DMF solutions ($10^{-3}$ M) using Jenway 4071 digital conductivity meter.

### *2.2. Synthesis of the ligand (HL)*

An ethanolic (20 ml) solution of re-crystallized *p*-anisidine (12.3 g, 0.1 mol) and acetyl acetone (10.2 ml, 0.1 mol) was taken in equimolar ratio in ethanolic media, then the mixture was refluxed for about 4 h on a water bath (80–90 °C) in the presence of few drops of piperidine as the condensing agent (Cumbal et al., 2007). The reaction mixture on ice-cooling gave an orange-yellow semi-solid which was preserved in a desiccator. Yield 60% (m.p. 86 °C).

### *2.3. Synthesis of complexes*

An ethanolic solution and 20 ml of (HL) Schiff base (2.05 g, 0.01 mol) were mixed with $CrCl_3{\cdot}6H_2O$, $MnCl_2{\cdot}4H_2O$, $CoCl_2{\cdot}6H_2O$, $NiCl_2{\cdot}6H_2O$ or $CuCl_2{\cdot}2H_2O$ (0.005 mol) in ethanol (20 ml) and the mixture was then refluxed for 2 h on a water bath (80–85 °C). The refluxed material was concentrated and cooled at 0 °C (Scheme 1). The colored solid products were filtered, washed with ethanol, and dried under vacuum. The preparation of metal complexes was shown in Scheme 2.

**Table 1** Physical properties of purolite S-930 resin.

| Purolite S-930 | |
|---|---|
| Matrix | Macro porous styrene–divinyl benzene |
| Functional group | Iminodi acetic acid |
| Purolite size (mm) | 0.3–1.0 |
| Bed density (g/L) | 710–745 |
| Particle density | 1.17 |
| Moisture content (%) | 55–65 |
| Operating tempters (max °C) | 70 |
| pH range (operating) | $H^+$ form 2–6, $Na^+$ form 6–11 |
| Total capacity (meq/ wet) | $H^+$ form 1.52, $Na^+$ form 1.29 |

### *2.4. Preparation of resins*

Prior to use, the resins were rinsed with de-ionized water to remove all impurities followed by a re-generation process to clean and convert the resin into H and Na form. The re-generation process involved washing the resin with 2 M HCl for 1 h, followed by de-ionized water rinse. The H-form resin was dried at 50 °C for 3 h. To convert the resin into Na-form, the resin was contacted with 2 M NaOH for 1hour followed by de-ionized water rinse. The resin was dried and stored at room temperature. The physical and chemical properties of the cationic H-form and Na-form resins are summarized in Table 1.

### *2.5. Calibration graph*

A three standard calibration graph for complex solutions in the concentration range of 20–120 ppm was prepared and used to determine the concentration of these complexes. Using the method of Least Squares (Miller and Miller, 2000), the regression equation [$Y = Xb \pm a$, where $b$ is the slope = 0.001876, 0.0026457 and 0.00355, $a$ is the intercept = −0.00982, −0.001587 and −0.003 for A1, A2 and A3 complexes, respectively, $X$ is the concentration, $Y$ is the absorbance] was utilized for the calculation of unknown concentration in samples. The validity of the regression equation was tested by analyzing the laboratory sample preparation. Beers law is valid within the concentration ranges of samples calculated.

### *2.6. Batch equilibrium adsorption*

Adsorption tests were carried out by the batch technique at 25 °C in a 250 ml tank reactor. The general method of adsorption involved adding and equilibrating 3 g of dry H or Na-form purolite S-930 resin or charcoal with 100 ml of metal complex solution A1 to A3 at various concentrations was agitated in shaker–incubator for 24 h at 400 rpm. The complex adsorbed concentration in solution was measured by UV–Vis spectrophotometer. An aliquot of the resulting aqueous solution was taken and assayed for the complex adsorbed concentration by reading the absorbance at $\lambda_{max}$ of the adsorption spectrum for initial and after adsorption solutions.

**Table 2** Physical properties and elemental analysis of the prepared compounds.

| Compound | Color/m.p. °C | Formula | Calc. (found) | | | |
|---|---|---|---|---|---|---|
| | | | C% | H% | N% | M%[a] |
| HL | Yellow/86–88 | $C_{12}H_{15}NO_2$ | 70.24 (70.40) | 7.31 (8.4) | 6.82 (7.2) | – |
| CrL | Pale yellow/201–203 | $\{CrL_2(H_2O)_2\}Cl$ | 54.08 (53.91) | 6.009 (5.91) | 5.25 (5.26) | 9.95 (10.01) |
| MnL | Pale pink/215–217 | $\{MnL_2(H_2O)_2\}$ | 57.71 (56.81) | 6.41 (5.11) | 5.61 (6.00) | 11.51 (10.29) |
| CoL | Green/209–211 | $\{CoL_2\}$ | 61.03 (62.11) | 6.38 (6.51) | 5.58 (5.81) | 11.98 (10.91) |
| NiL | Red/213–215 | $\{NiL_2\}$ | 60.91 (59.1) | 6.0 (6.91) | 4.99 (5.71) | 12.44 (12.39) |
| CuL | Red/217 d | $\{CuL_2\}$ | 61.08 (60.9) | 6.30 (7.1) | 5.51 (5.91) | 12.51 (13.64) |

d = Decomposed.

[a] Analysis of metal percentage via F.A.A.S.

## 3. Results and discussion

The analytical data along with some physical properties of the complexes are summarized in Table 2. The analytical data show that the [M:L] ratio is 1:2 They are non soluble in common organic solvents except DMF and DMSO. The Low molar conductance values of the complexes reveal their non-electrolytic nature except Cr(III) complex which show electrolytic behavior in 1:1 ratio (Cumbal et al., 2007) supporting their formulation on the bases of the chemical analysis.

### *3.1. Analysis*

A three standard calibration graph for complexes solutions Fig. 1 in the concentration range 20–120 ppm was used to determine the concentration of these complexes. In order to examine the accuracy and precision of the analysis method, Table 3 summarizes the analysis of the laboratory sample, the results show the relative error ranging from ±1.08 to 5.31, ±1.04 to 4.82 and ±0.28 to 3.09 and the relative standard deviation did not exceed ±6.23%, ±2.77% and ±4.38% for A1, A2 and A3 complexes, respectively, Table 4, Chart 1.

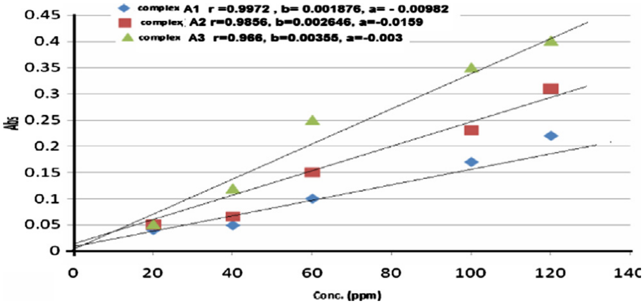

**Figure 1** Standard calibration graph for (A1–A3) complexes solution.

### *3.2. IR spectra*

Table 5 described the characteristic stretching vibrations exhibited by the Schiff base (HL) and their metal complexes. Three distinct absorptions related to the free ligand were observed and assigned to $\upsilon_{C=O}$, $\upsilon_{OH}$ and $\upsilon_{C=N}$, respectively, Figs. 2–6. The first band appeared in the free ligand (HL) at 1697 $cm^{-1}$ with a shoulder at 1625 $cm^{-1}$ was assigned to $\upsilon_{C=N}$ of the Schiff base (Raman et al., 2004). The presence

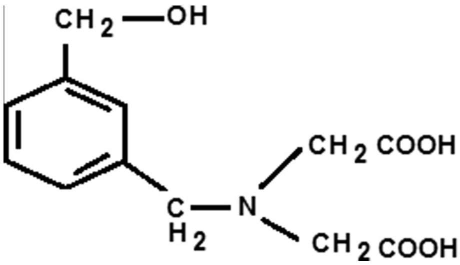

**Chart 1** Chemical structure of purolite S930 (H-Form).

**Table 3** Analysis of standard laboratory complex solution samples, 50 ppm.

| Complex | Sample no. | Abs. | Conc. (ppm) | Average conc. (ppm) | Absolute error | Relative error (%) |
|---|---|---|---|---|---|---|
| A1 | 1 | 0.088 | 52.143 | 49.6373 | −2.143 | 4.286 |
| | 2 | 0.081 | 48.412 | | +1.58 | 3.16 |
| | 3 | 0.079 | 47.345 | | +2.655 | 5.31 |
| | 4 | 0.085 | 50.544 | | −0.544 | 1.088 |
| ∑ | | | 198.55 | | | |
| A2 | 1 | 0.110 | 47.59 | 49.86 | +2.41 | 4.82 |
| | 2 | 0.118 | 50.615 | | −0.615 | 1.23 |
| | 3 | 0.121 | 51.746 | | −1.747 | 3.494 |
| | 4 | 0.115 | 49.478 | | +0.5217 | 1.043 |
| ∑ | | | 199.44 | | | |
| A3 | 1 | 0.180 | 51.549 | 50.5634 | −1.549 | 3.09 |
| | 2 | 0.175 | 50.141 | | −0.1408 | 0.2816 |
| | 3 | 0.178 | 50.986 | | −0.986 | 1.972 |
| | 4 | 0.173 | 49.577 | | +0.4225 | 0.845 |
| ∑ | | | 202.254 | | | |

**Table 4** Method precision and accuracy.

| Average conc. (ppm) | | S.d | R.S.d% | S.d of the mean | R.S.d% of the mean |
|---|---|---|---|---|---|
| A1 | 29.991 | 1.869 | ±6.23 | 0.934 | ±3.116 |
| A2 | 43.43 | 1.2 | ±2.77 | 0.6 | ±1.38 |
| A3 | 33.177 | 1.454 | ±4.383 | 0.727 | ±2.191 |

**Table 5** IR spectral data of the ligand and it' s metal complexes ($\upsilon$ cm$^{-1}$).

| Compound | $\upsilon$C = 0, OH | $\upsilon$C = N | M–N, M-0 | Other bonds |
|---|---|---|---|---|
| HL | 1697(s), 3400–3209 (br) | 1625(s), 1590–1481(m) | – | 1234 (C–O) |
| Cr$^{III}$L | 3425(br)[a] | 1620(s), 1519–1458(m) | 523, 401 (w) | 632 (w), 941[b] |
| MnL | 3288(br)[a] | 1666–1635(s), 1608(m) | 534 (w), 445 (w) | 655–947 (w)[b] |
| CoL | – | 1620(s),1514(m) | 555(br), 470 (w) | 1280 (C–O) |
| NiL | 1644(s) | 1595(s), 1535(s) | 530 (m), 430 (w) | 1275 (C–O) |
| CuL | 1639(s) | 1585(s), 1570(s) | 578 (m), 422 (w) | 1262 (C–O) |

br = Broad, s = strong, m = medium and w = weak.

[a] Broad vibrational mode of coordinated $H_2O$ molecules in Cr(III) and Mn(II) complexes.

[b] Rocking of O–H for $H_2O$ coordinated to Cr(III) and Mn(II).

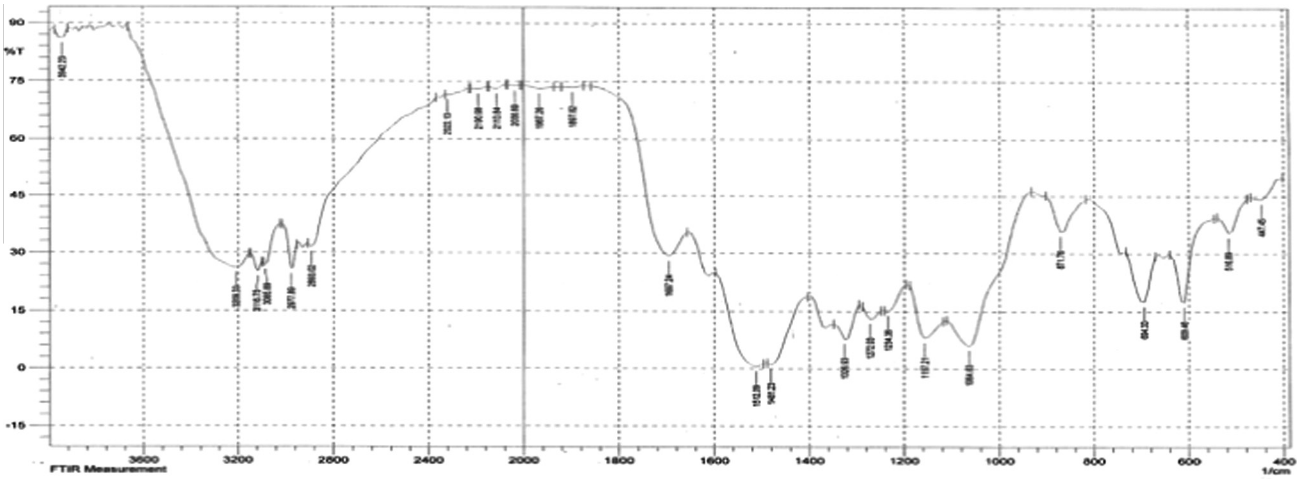

**Figure 2** FT-IR spectrum of HL ligand in KBr disc.

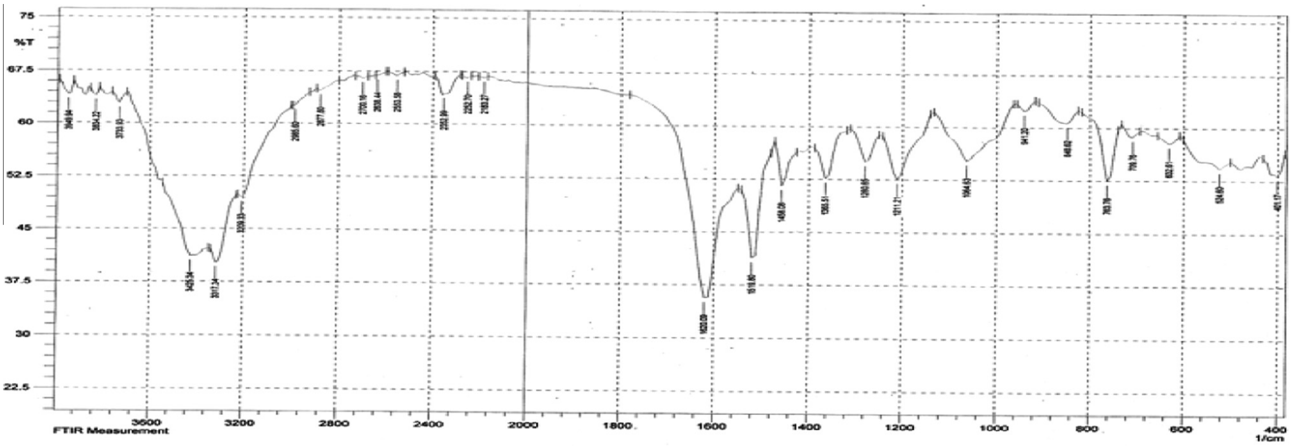

**Figure 3** FT-IR spectrum of Cr$^{III}$–L complex in CsI-disc.

of two absorption bands at 1697 cm$^{-1}$ (C═O) and a broad band at 3400 cm$^{-1}$ confirms the existence of keto and enol forms of the ligand (Silversten and Webster, 1998). Complexation of metal ions to the Schiff base shifted the bands of C═O and C═N to lower frequencies, this means that the bond order of C═O and C═N decreased due to the formation of M–N and M–O bonds (NeKamto, 1997). As well as the disappearance of broad absorptions at 3400–3205 cm$^{-1}$ in the formed complexes investigates the deprotonation of –OH group, Figs. 3 and 4 (Ferraro, 1971). The inspection of the bands due to C═O and C═C stretching frequencies showed a small relative change in the position companied by reduction in the intensity. The bands attributed to M–N and M–O were observed in the regions 405–432 cm$^{-1}$ and 410–530 cm$^{-1}$,

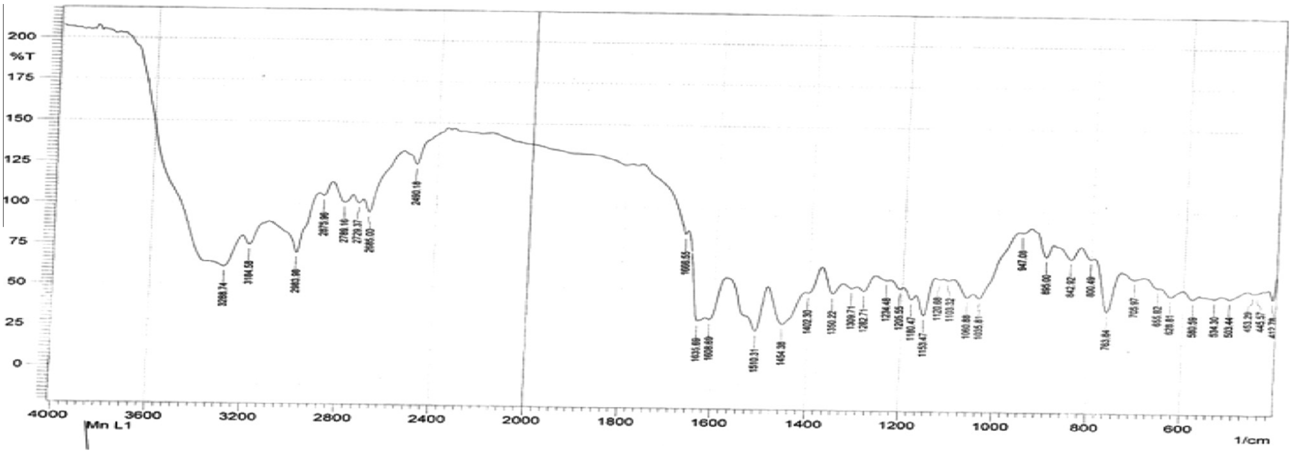

**Figure 4** FT-IR spectrum of Mn$^{II}$–L complex in CsI-disc.

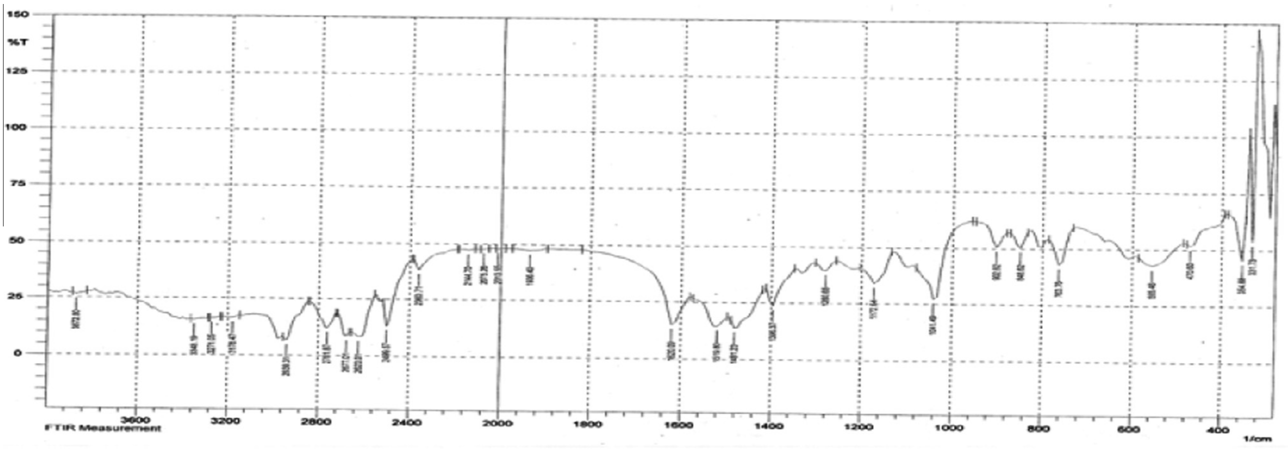

**Figure 5** FT-IR spectrum of Co$^{II}$–L complex in CsI-disc.

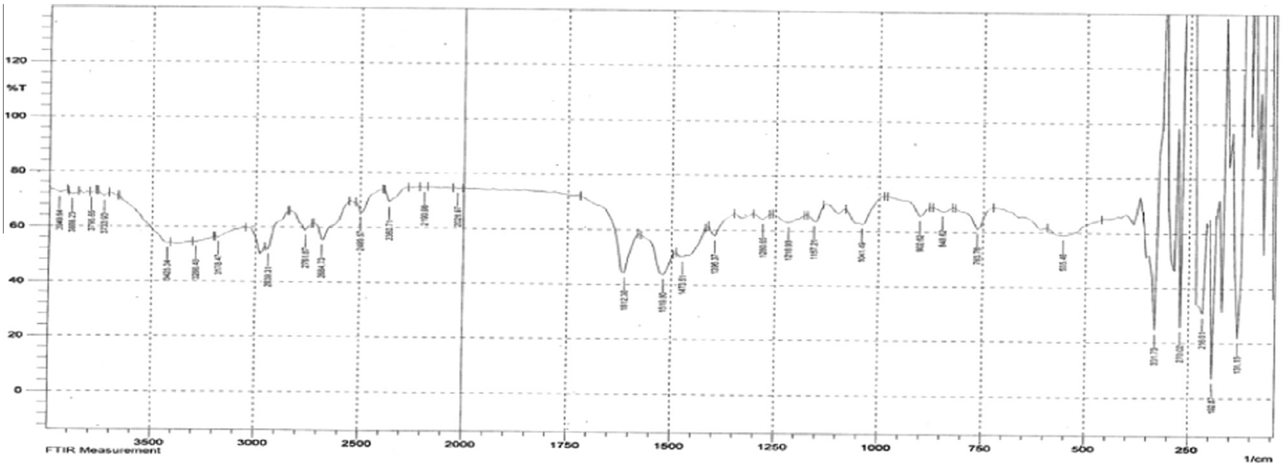

**Figure 6** FT-IR spectrum of Cu$^{II}$–L complex in CsI-disc.

respectively (Natarajan and Agarwala, 1978; Mishra and Chaturvedi, 1994). The infrared spectra of Cr$^{III}$ and Mn$^{II}$ complexes show additional bands at 3425, 3288 and 632–947 cm$^{-1}$ which are assignable to the vibration of O–H and rocking of coordinated water molecule (Geary, 1971).

### *3.3. Electronic spectra, magnetic moment and conductivity measurements for the metal complexes*

The electronic spectra of the Schiff base (HL) and their complexes were recorded in ethanol and DMF as solvent at room

**Table 6** UV–Vis spectra data, magnetic moments and molar conductivity measurements for the prepared complexes.

| Compound | Absorbtion (υ cm$^{-1}$) | Assignment | $\mu_{\text{eff}}$ (B.M) | □, [a] S cm$^2$ ml$^{-1}$ | Geometry |
|---|---|---|---|---|---|
| HL | 35,810 | INCT | – | – | – |
| | 28,011 | $n \rightarrow \pi$[a] | | | |
| Cr$^{III}$L | 17,850 | $A_2^4g \rightarrow T_2^4g$ | 3.05 | 185 | Octahedral |
| | 21,520 | $A_2^4g \rightarrow T_1^4g(F)$ | | | |
| Mn$^{II}$L | 37,313 | $A_1^6g \rightarrow T_1^4g(p)$ | 3.5 | 25 | Octahedral |
| | 15,625 | $A_1^6g \rightarrow T_1^4g(G)$ | | | |
| Co$^{II}$L | 29,950 | INCT | 2.10 | 18 | Square planner |
| | 16,390 | $A_1^2g \rightarrow E_1^1g$ | | | |
| Ni$^{II}$L | 38,950 | INCT | 0 | 20 | Square planner |
| | 19,550 | $A_1^1g \rightarrow B_1^1g$ | | | |
| Cu$^{II}$L | 33,660 | $B_1^2g \rightarrow A_1^2g$ | 1.51 | 30 | Square planner |
| | 21,881 | | | | |

INCT = Intra-ligand charge transfer.

[a] Molar conductance measurements were carried out in $10^{-3}$ M solution of DMF.

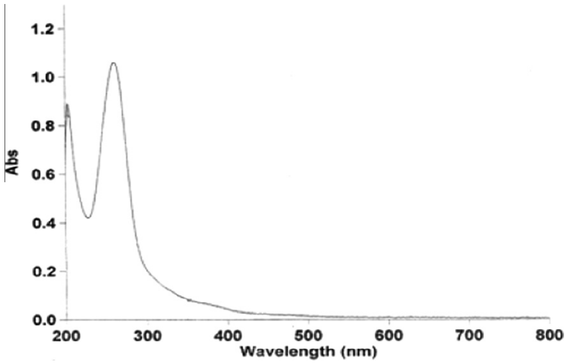

**Figure 7** UV–Vis spectra of HL in ethanol ($10^{-3}$ M conc.).

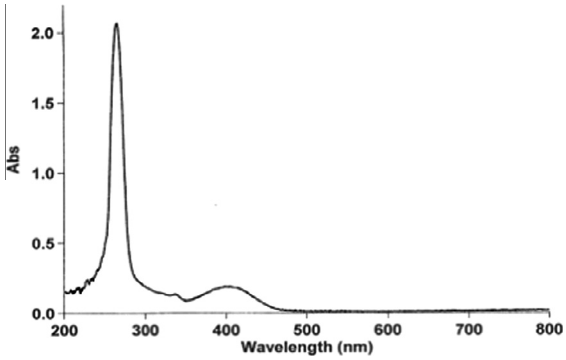

**Figure 9** UV–Vis spectra of Cu$^{II}$ complex in DMF ($10^{-3}$ M conc).

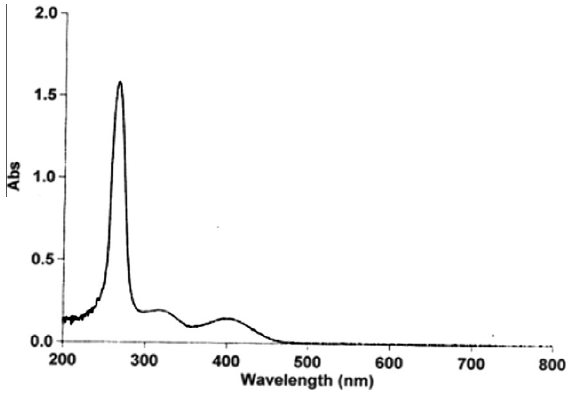

**Figure 8** UV–Vis spectra of Ni$^{II}$ complex in DMF ($10^{-3}$ M conc.).

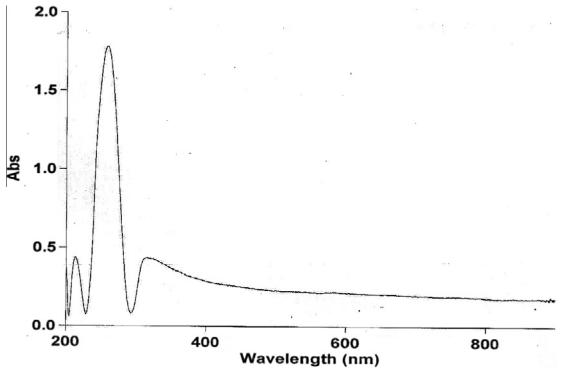

**Figure 10** UV–Vis spectra of Co$^{II}$ complex in DMF ($10^{-3}$ M conc).

temperature, the UV–Vis, molar conductivity and magnetic susceptibilities of (HL) complexes are described in Table 6, Figs. 7–10. The isolated complexes are stable in air, completely insoluble in water and common organic solvents, but completely soluble in DMF and DMSO. The analytical data, Table 2, indicate that the complexes are mononuclear in nature. The molar conductance values measured in DMF solution ($10^{-3}$ mol dm$^{-3}$) fall in the range 18–30 Ω$^{-1}$ cm$^2$ mol$^{-1}$ for Mn(II), Co(II), Ni(II) and Cu(II). These observed values of the molar conductance are well within the expected range for non-electrolytes (Geary, 1971). However, the Cr(III) complex solution ($10^{-3}$ M) in DMF exhibits electrolytic behavior in 1:1 ratio which confirms the ionic forms of the proposed formula $[CrL_2(H_2O)_2]^+ Cl^-$ (Burger, 1973). The Cr(III) complex shows a magnetic moment corresponding to three unpaired electrons (3.01BM), which is approximately equal to spin-only value (Satyanarayana, 2001). The band at 17,850 and 21,520 cm$^{-1}$ in the Cr(III) complex is assignable to the transitions from $A_2^4g(F) \rightarrow T_2^4g(F)$ and $A_2^4g(F) \rightarrow T_1^4g(P)$, respectively, also the various electronic parameters, i.e. 10Dq = 17,850 cm$^{-1}$, $B = 498.836$ cm$^{-1}$, $V_2/V_1 = 1.20$, and $\beta = 0.475$ are in fair agreement with octahedral structure of the Cr(III) complex (Satyanarayana, 2001). The low value of *nepheloauxetic* effect indicates the covalent character of M–L bond. The spectrum of light pink (d$^5$) Mn(II)-complex exhibited absorption bands at 37,878 cm$^{-1}$ and 15,625 cm$^{-1}$ belonging to $A_1^6g \rightarrow T_1^4g(p)$ and $A_1^6g \rightarrow T_1^4g(G)$ (Lever, 1984). The magnetic moment of Mn(II) complex equal to (3.50 BM) falls in the range reported for low spin ($S = 1/2$) octahedral Mn(II) complex (Kumar and Chandra, 2006). These rules together with the data of UV–Vis spectra are accepted for Mn(II) octahedral complexes. The Ni(II) complex is diamagnetic, suggesting the square planner geometry around nickel ion. The electronic spectrum of the red solution of Ni(II) complex in DMF solution displayed absorption bands at 38,950 cm$^{-1}$ and 19,550 cm$^{-1}$ . These bands may be assigned to the INCT and $A_1^1g \rightarrow B_1^1g$ transitions, respectively (Abdul Ghani and Tapashi, 1990). The electronic spectrum of Cu(II) complex shows bands at 33,660 cm$^{-1}$ and 21,881 cm$^{-1}$. These bands corresponded to the transitions CT and $B_2^1g \rightarrow A_1^2g$, respectively (Duward and Atkins, 1990). As well as Co(II) complex exhibited high intensity band at 29,950 cm$^{-1}$ and low intensity band in the visible region, 16,390 cm$^{-1}$. These transitions may be attributed to INCT and $A_1^1g \rightarrow B_1^1g$, respectively (Duward and Atkins, 1990). The position of these bands together with magnetic moments value for Cu(II), Ni(II) and Co(II) complexes confirms the square planar geometry (Dunn, 1960), Tables 7–9.

### 3.4. Batch adsorption

The batch adsorption tests were carried out in a 250 ml reactor, shaking at 400 rpm for 24 h, this period was sufficient to attain equilibrium adsorption. The complex concentration of adsorption was determined using atomic absorption spectroscopy or UV–Vis at $\lambda_{max}$ of the adsorption spectrum. The adsorption capacity ($Q_e$) of the resins per unit mass was calculated from the following equation:

$$Q_e = \frac{C_i - C_e}{m} V \tag{4}$$

where $C_i$ and $C_e$ are the initial and equilibrium concertinos at metal complex (mg/L), $V$ is the volume of metal complexes solutions (L) and $m$ is the weight of dry resin (g).

**Table 7** Adsorption parameters complexes of ($A_1$) on adsorbents.

| Surface | $C_e$ ppm | Abs. 1 | $C_e$ ppm | Abs. 2 | $Q_e = x/m$ | log $x/m$ | log $C_e$ | $C_e/Q_e$ |
|---|---|---|---|---|---|---|---|---|
| Charcoal | 20 | 0.133 | 14.6 | 0.096 | 10.6 | 1.029 | 1.161 | 1.37 |
| | 40 | 0.26 | 29.31 | 0.18 | 21.2 | 1.31 | 1.459 | 1.38 |
| | 60 | 0.39 | 45 | 0.28 | 31.4 | 1.6 | 1.68 | 1.43 |
| | 80 | 0.645 | 72.9 | 0.5 | 53.1 | 1.71 | 1.86 | 1.37 |
| | 20 | 0.133 | 19.3 | 0.12 | 1.4 | 0.146 | 1.29 | 13.70 |
| $R^+$ | 40 | 0.261 | 39 | 0.25 | 2.9 | 0.521 | 1.61 | 13.40 |
| | 60 | 0.389 | 57.1 | 0.35 | 5 | 0.613 | 1.8 | 11.42 |
| | 80 | 0.517 | 90.3 | 0.55 | 6.5 | 0.755 | 1.955 | 13.80 |
| | 20 | 0.133 | 14.8 | 0.099 | 10.3 | 1.05 | 1.21 | 1.43 |
| $R^-$ | 40 | 0.27 | 29.3 | 0.21 | 22.1 | 1.71 | 1.51 | 1.32 |
| | 60 | 0.4 | 45.3 | 0.31 | 33.61 | 1.99 | 1.92 | 1.34 |
| | 80 | 0.71 | 66.7 | 0.503 | 49.3 | 2.03 | 2.01 | 1.35 |

$R^+$ = cationic H-form purolite S-930 resin and $R^-$ = Na-form purolite S-930 resin.

**Table 8** Adsorption parameters complexes of ($A_2$) on adsorbents.

| Surface | $C_e$ (ppm) | Abs 1 | $C_e$ (ppm) | Abs.2 | $Q_e = x/m$ | log $x/m$ | log $C_e$ | $C_e/Q_e$ |
|---|---|---|---|---|---|---|---|---|
| Charcoal | 20 | 0.063 | 16.3 | 0.053 | 7.2 | 0.88 | 1.22 | 2.26 |
| | 40 | 0.127 | 32.1 | 0.160 | 15 | 1.60 | 1.66 | 2.14 |
| | 60 | 0.192 | 48.1 | 0.150 | 22.1 | 1.4 | 1.8 | 2.17 |
| | 80 | 0.260 | 86.1 | 0.230 | 27 | 1.8 | 1.99 | 3.18 |
| | 20 | 0.063 | 17.2 | 0.055 | 5.7 | 0.757 | 1.235 | 3.01 |
| $R^+$ | 40 | 0.127 | 35.1 | 0.109 | 11.4 | 1.05 | 1.53 | 3.07 |
| | 60 | 0.192 | 51.5 | 0.165 | 17.2 | 1.234 | 1.77 | 2.99 |
| | 80 | 0.320 | 85.7 | 0.275 | 28.7 | 1.5 | 2.01 | 2.98 |
| | 20 | 0.040 | 33.2 | 0.057 | 13.4 | 1.12 | 1.53 | 2.47 |
| $R^-$ | 40 | 0.072 | 47.3 | 0.080 | 20.16 | 1.3 | 1.7 | 2.34 |
| | 60 | 0.104 | 60.2 | 0.110 | 26.88 | 1.419 | 1.85 | 2.23 |
| | 80 | 0.166 | 83.7 | 0.192 | 33.6 | 1.53 | 2 | 2.44 |

$R^+$ = cationic H-form purolite S-930 resin and $R^-$ = Na-form purolite S-930 resin.

**Table 9** Adsorption parameters complexes of ($A_3$) on adsorbents.

| Surface | $C_e$ (ppm) | Abs 1 | $C_e$ (ppm) | Abs.2 | $Q_e = x/m$ | log $x/m$ | log $C_e$ | $C_e/Q_e$ |
|---|---|---|---|---|---|---|---|---|
| Charcoal | 20 | 0.034 | 16.1 | 0.03 | 7.8 | 0.892 | 1.202 | 2.06 |
| | 40 | 0.072 | 32.1 | 0.052 | 15.6 | 1.193 | 1.108 | 2.05 |
| | 60 | 0.104 | 48.1 | 0.077 | 23.6 | 1.369 | 1.684 | 2.04 |
| | 80 | 0.168 | 80.5 | 0.124 | 34 | 1.591 | 1.906 | 2.36 |
| $R^+$ | 20 | 0.04 | 19.48 | 0.031 | 1.04 | 0.017 | 1.28 | 18.73 |
| | 40 | 0.072 | 38.96 | 0.062 | 2.07 | 0.318 | 1.519 | 18.82 |
| | 60 | 0.104 | 58.44 | 0.094 | 3.20 | 0.494 | 1.76 | 18.26 |
| | 80 | 0.168 | 97.4 | 0.155 | 5.20 | 0.716 | 1.99 | 18.73 |
| $R^-$ | 20 | 0.040 | 16.64 | 0.026 | 6.71 | 0.821 | 1.23 | 2.40 |
| | 40 | 0.070 | 33.21 | 0.057 | 13.5 | 1.123 | 1.561 | 2.47 |
| | 60 | 0.104 | 49.19 | 0.08 | 20.10 | 1.411 | 1.711 | 2.23 |
| | 80 | 0.168 | 83.21 | 0.133 | 33.4 | 1.61 | 1.999 | 2.49 |

$R^+$ = cationic H-form purolite S-930 resin and $R^-$ = Na-form purolite S-930 resin.

### *3.5. Metal complexes adsorption by adsorbent surfaces*

The adsorption on the surfaces increased with increasing of the adsorbent amount. All the surfaces tested can adsorb Cr(III), Mn(II) and Co(II) complexes. Figs. 11–16 depict the adsorption isotherms for (A1–A3) complexes on charcoal, H and Na-form puroline resins at 298 °K.

According to Freundlich equation, the adsorption percentage of Cr(III) complex (A1) is ≈96% compared with other complexes A2 and A3 since CrL complex behaves as a electrolytic species in ratio 1:1, therefore the ions exchange on the surface of H-form and Na-form of S-930 resin compared with charcoal surface. Carboxylic group $(CH_2CO_2H)_2$ on purolite S-930 surface is generally known to have a strong interaction with Cr(III)–A1 complex (Rochester, 1980). The competitive adsorption of several metal ions present in A1–A3 complexes, Cr(III), Mn(II) and Co(II) in 20–120 ppm each one on 3 g surface revealed that the H and Na-form S-930 resins exhibited strong affinity with A3 complexes while A2 and A3 complexes exhibited the strongest affinity with charcoal which is considered a physical adsorption (Nasiruddin, 2004). In general, electrostatic adsorption of Cr(III), Mn(II), and Co(II) complexes is influenced by pH because the forms of metal ions and their ionic changes depended on pH. Adsorption of Cr(III), Mn(II) and Co(II) complexes decreased above pH (8–11) for Na-form profited, but adsorption of A1–A3 complexes decreased below for H-form of purolite S-930 (Tella and Owaludu, 2007). The Freundlich expression is an equation based on sorption on a heterogeneous surface suggesting that binding site is not equivalent and /or independent. According to the linear logarithmic form of Freundlich adsorption equation number 5 (Vadi et al., 2010; Muthulakshmi and Sakthi, 2010):

$$\log \frac{X}{m} = \frac{1}{n} \log C_e + \log K \qquad (5)$$

The Freundlich constants ($K$) and ($n$) related to the sorption capacity and sorption intensity of the sorbent, respectively, were calculated for each adsorbent (charcoal, $H^+$ and $Na^+$ form purolite S-930), Table 10. Figs. 9–14 show Langmuir and Frendlich adsorption isotherms of A1–A3 complexes on precious adsorbents. From these studies, it is observed that the % adsorption agrees with Freundlich adsorption capacity ($K_f$). The concentration of Cr(III) metal complexes in equilibrium increases with $Q_e$ which obeys the ionic exchange theory of H and Na-form purolite S-930 (Goto, 2007).

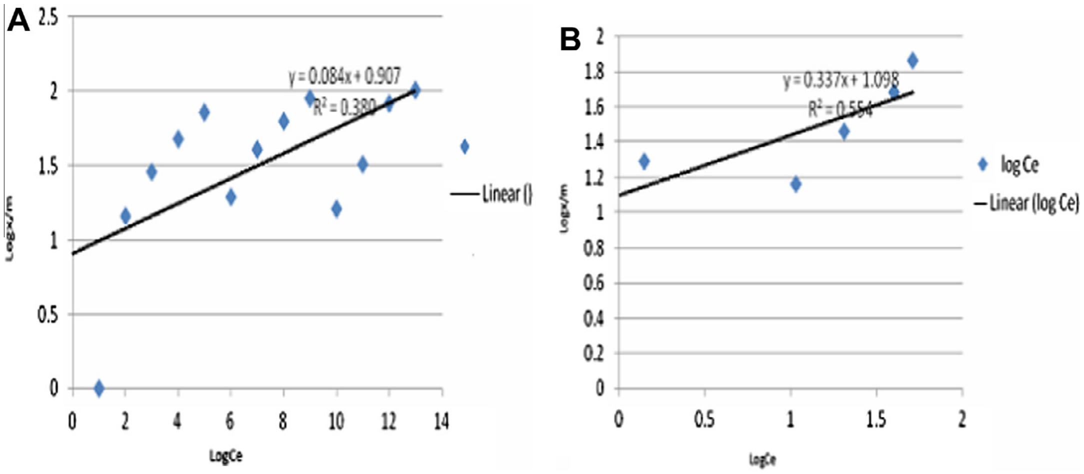

**Figure 11** Freundlich adsorption isotherm plot for A1 complex (A: purolite S930 H+ form, B: charcoal complex).

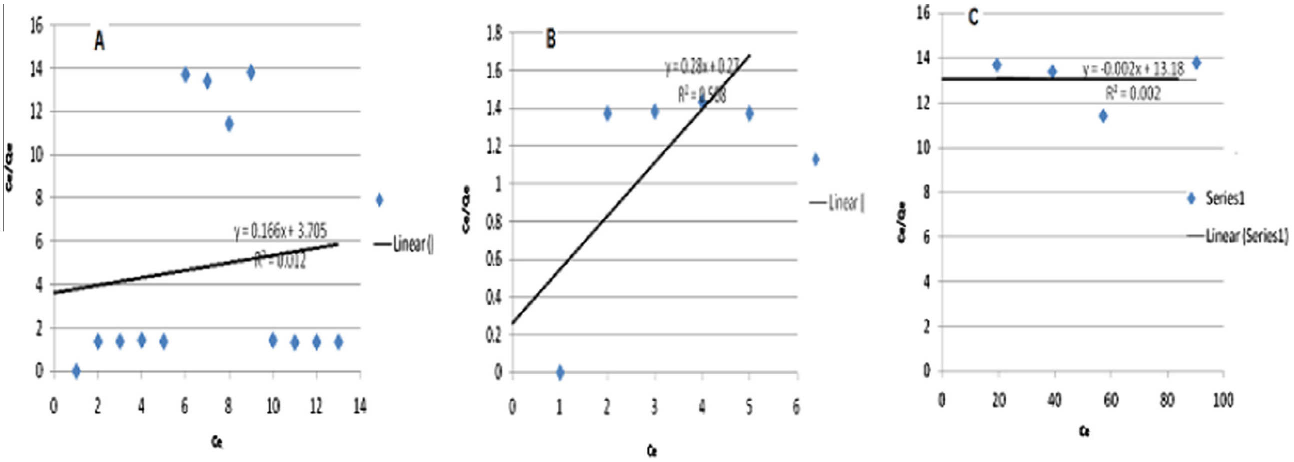

**Figure 12** Langmuir adsorption isotherm plot for A1 complex (A: charcoal, B: $H^+$ form purolite, C: $Na^+$ form purolite).

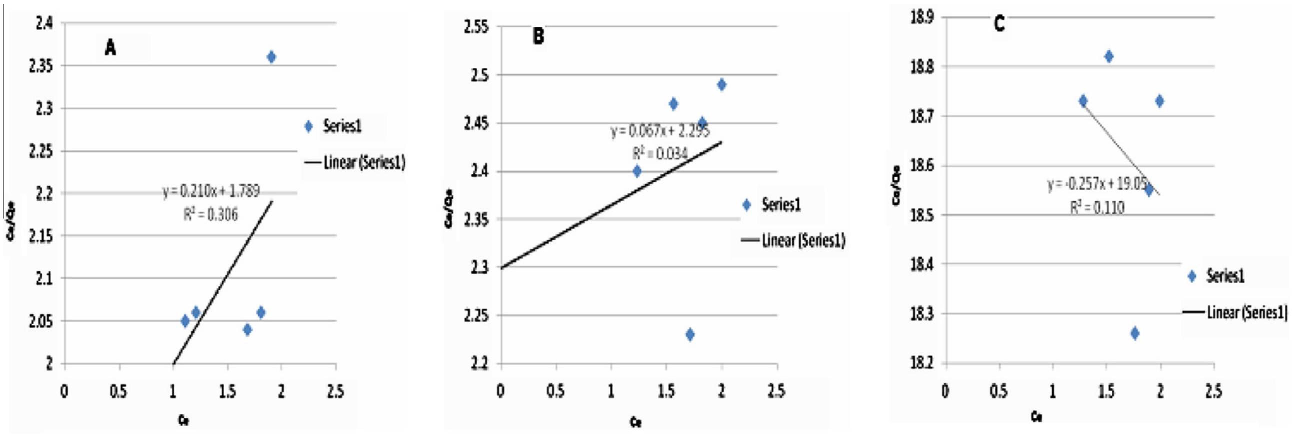

**Figure 13** Langmuir adsorption isotherm plot for A2 complex (A: charcoal, B: $H^+$ form purolite, C: $Na^+$ form purolite).

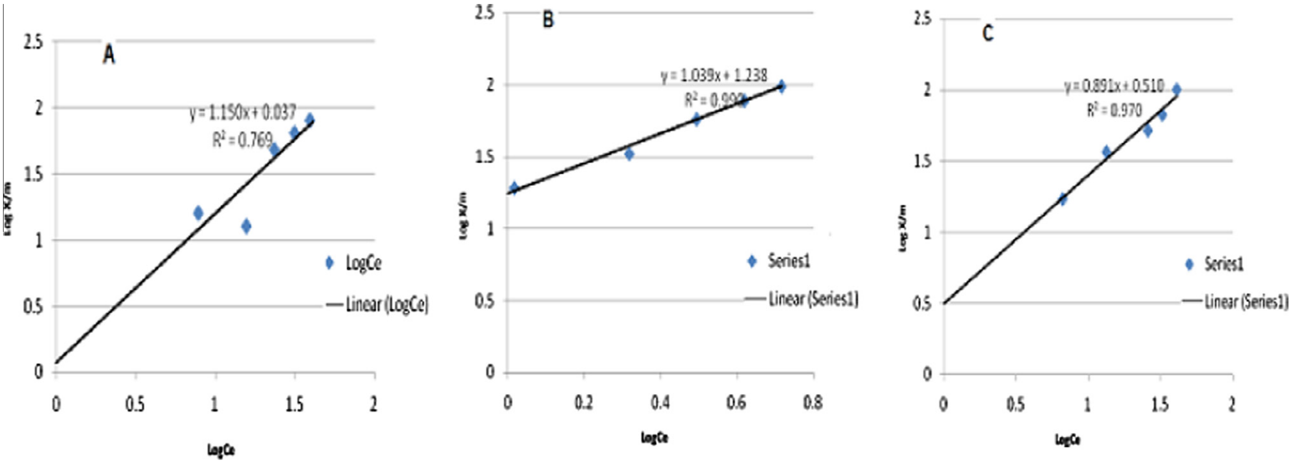

**Figure 14** Freundlich adsorption isotherm plot for A2 complex (A: charcoal, B: $H^+$ form purolite, C: $Na^+$ form purolite).

The numerical value $(1/n) < 1$ for charcoal and $R^+$ for A3 complex indicates that adsorption capacity is only slightly suppressed at lower equilibrium concentrations. This adsorption isotherm doesnot predict any saturation of the sorbent by the sorbate, thus infinite surface coverage is mathematically predicted, indicating multilayer adsorption on the surface (Matejka and Weber, 1990), However, the rate constant adsorption (Kd) and adsorption percentage were calculated, Table 10, these results indicate that Cr(III) complex has polar structure and low surface area due to higher adsorption per-

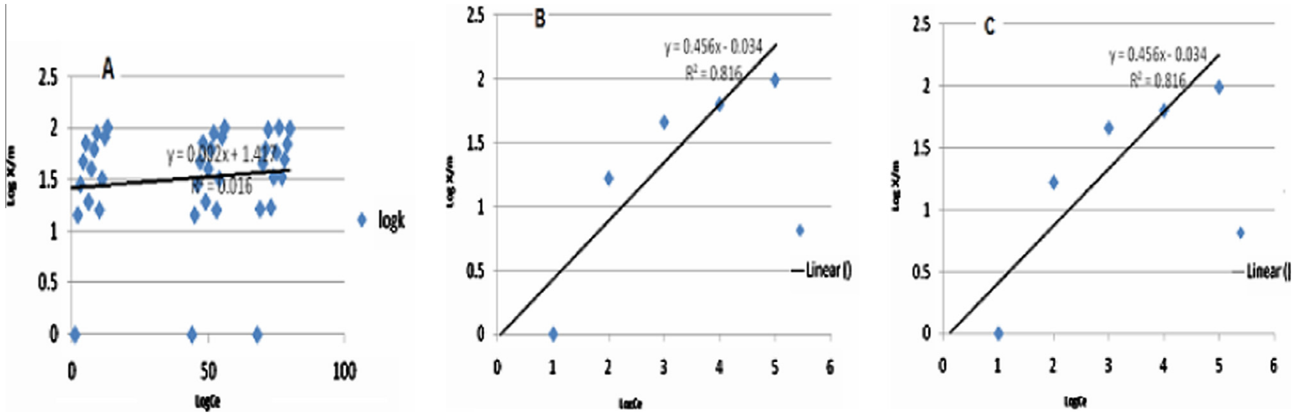

**Figure 15** Freundlich adsorption isotherm plot for A3 complex (A: charcoal, B: $H^+$ form purolite, C: $Na^+$ form purolite).

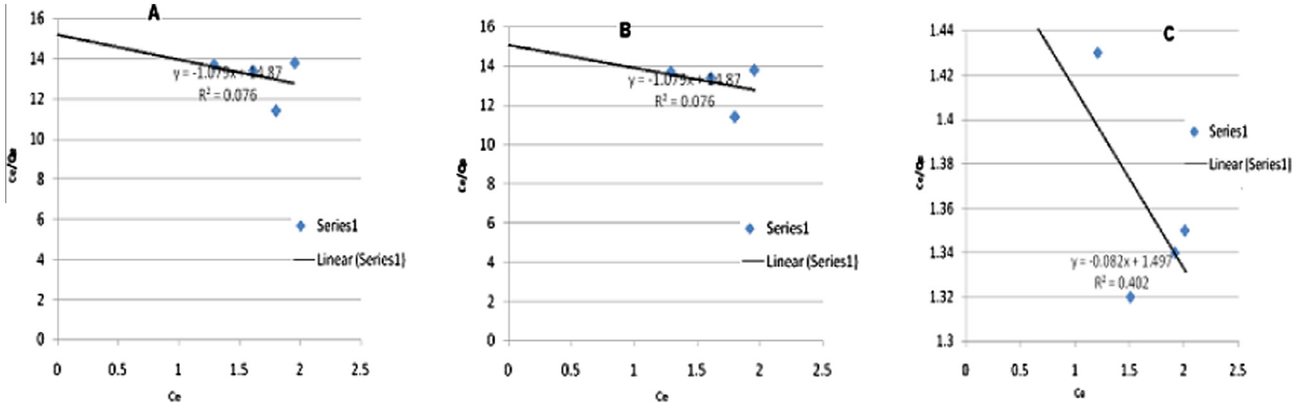

**Figure 16** Langmuir adsorption isotherm plot for A3 complex (A: charcoal, B: $H^+$ form purolite, C: $Na^+$ form purolite).

**Table 10** Adsorption parameter of $A_1$ –$A_3$ Complexes.

| Complex | Adsorbent | % Adsorption | $K$ (ml/g) | $1/n$ | log $k$ |
|---|---|---|---|---|---|
| $A_1$ | Charcoal | 40.84 | 20.4 | 0.91 | 0.081 |
| | $R^+$ | 90 | 16.2 | 1.03 | 1.80 |
| | $R^-$ | 85 | 19 | 1 | 0.14 |
| $A_2$ | Charcoal | 80 | 16.7 | 0.99 | 0.17 |
| | $R^+$ | 4.3 | 2.3 | 1.009 | −1.05 |
| | $R^-$ | 34.2 | 17.5 | 1.02 | −0.17 |
| $A_3$ | Charcoal | 36.21 | 18.12 | 0.97 | −0.139 |
| | $R^+$ | 3.71 | 1.91 | 0.81 | −1.21 |
| | $R^-$ | 27.51 | 17.9 | 1.5 | −1.63 |

$R^+$ = cationic H-form purolite S-930 resin and $R^-$ = Na-form purolite S-930 resin.

centage as well as the high value of (1/n) indicates the high affinity of H and Na-form purolite S930 toward Cr(III) rather than neutral complexes of Mn(II) and Co(II) (Matejka and Weber, 1990). Linear plot of log $Q_e$ versus log $C_e$ showed that the adsorption isotherm of these three complexes on activated carbon and H and Na-forms of purolite S-930 surface obeys Freundlich isotherm and was similar to (S-curve) type according to Giles classification (Levine Ira, 1988) which investigates the heterogeneous adsorption (Levine Ira, 1988). The regression values indicate that the adsorption data for these complexes fitted well within the Freundlich isothermal plots for the concentration studied.

## 4. Conclusion

We have synthesized Cr(III), MN(II), Co(II), Ni(II) and Cu(II) complexes using the Schiff base (HL) formed by the condensation of acetyl acetone and *p*- anisidine. The complexes were characterized by spectral, magnetic and conductivity studies to establish the proposed four-coordinated square-planner geometry around Co(II), Ni(II) and Cu(II) ions and six-coordinated octahedral geometry around MN(II) and Cr(III) ions. The (HL) ligand behaves as a monobasic bidentate chelating agent coordinating through protonated hydroxyl group and nitrogen atom of azomethine group, which forms kinetically stable six-membered ring with metal ion. It is further confirmed on the basis of considerable low value of magnetic moments in the case of Co(II), Ni(II) and Cu(II) complexes which reveal the low-spin square planar geometry. As well as the lower value of *nepheloauxetic* parameters gives Dq = 1785 $cm^{-1}$, $\beta'$ = 0.475 in Cr(III) complex which indicates a strong covalent nature of this metal–ligand σ-bond.

Purolite S-930 resins exhibit specific interaction with metal complexes. Here, we found that the exchange of (counter ions) for A1 complex interacts easily with the bulky structure of the resin according to the suggested equation:-

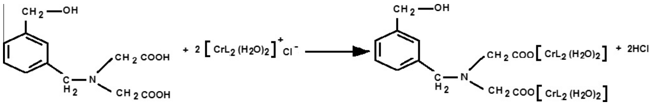

The wide range 2–6 for H-form and 6–11 for Na-form of purolite S-930 investigates the total capacity of such resin toward A1–A3 complex in aqueous solution. The Langmuir and Freundlich adsorbed complexes on charcoal and purolite S-930 resin, which reveals the heterogeneous adsorption via different forces, the force the adsorption energy which reduces with increasing the cover areas of surface.

## References

Abdul Ghani, A.T., Tapashi, N.O., 1990. Synthesis and characterization of *N*-2,4-dimethoxy benzylidene-2-hydroxy aniline and its complexes with some transition metal ions. Iraqi J. Chem. 27 (3), 649–663.

Burger, K., 1973. Coordination Chemistry Experimental Methods. Butt/worth and Co.(publishers) Ltd., London.

Cumbal, L., Greenleaf, J., Leun, D., SenGupto, A.K., 2007. Polymer supported inorganic nano particle; characterization and environmental application. Reactive Polym. 55, 180–186.

Dunn, T.M., 1960. The Ultraviolet and Visible Spectra of Complexes Compounds in Modern Coordination Chemistry. New York Interscience.

Duward, F.S., Atkins, P.W., 1990. Inorganic Chemistry. Oxford University Press.

Ferraro, J., 1971. Low Frequency Vibration of Inorganic Compound. Ed. Plenim, New York.

Freundlich, H.M.F., 1971. Over the adsorption in solution. J. Phys. Chem. 57, 385–470.

Geary, W.J. for the characterization of coordination compounds (1971)" The use of conductivity measurements in organic solvents. Coord. Chem. Rev. 7 (1), 81–122.

Goto, M., 2007. Utilization of natural found Waster as anew adsorbent for precious metal ions. Chem. Eng. J., 16–20.

Kumar, L., Chandra, S., 2006. Trans. Met. Chem. 31, 3687.

Langmuir, I., 1918. The adsorption of gases on plane surfaces of glass, mica and platinum. J. Am. Chem. Soc. 40, 1361–1403.

Lever, A., 1984. Inorganic Electronic Spectroscopy. Elsevier publishing, New York.

Levine Ira, N., 1988. Physical Chemistry, 3rd ed. McGraw-Hill Book Cop., Singapore, pp. 371–374.

Matejka, Z., Weber, R., 1990. Ligand exchange sorption of carboxylic and amino carboxylic anions by chelating resins loaded with heavy metal cations. Recent Polym. 13, 299–308.

Miller, James N., Miller, Jane C, 2000. Statistics and Chemometrics for Analytical Chemistry, 4th ed. Prentice Hall.

Mishra, S., Chaturvedi, M., 1994. J. Indian Council Chem. 10, 7.

Muthulakshmi, N., Sakthi, V., 2010. A comparative study on the sorption characteristics of Pb(II) and Hg(II) onto activated carbon. E-J. Chem. 7 (3), 967–974.

Nasiruddin, M., 2004. Adsorption removal of non-ionic surfactants from water wing granite sand. J. Iranian Chem. Soc. 1 (2), 152–158.

Natarajan, K., Agarwala, U.C., 1978. Inorg. Nucl. Chem. Lett. 14, 7.

NeKamto, K., 1997. Infrared and Raman spectra of Inorganic and Coordination Compounds. Wiley, New York.

Raman, N., Ravichandran, S., Thingaraja, C., 2004. Synthesis, characterization and biological activity of metal complexes with new Schiff bases of semicarbazone. J. Chem. Soc. 116, 215.

Ramana, A., Sengupta, A.K., 1992. A new class of selenium axyanions. Environ. Eng. Div. J. Asc. E118 (5), 755, 755.

Rochester, C.H., 1980. Adv. Collid. Interface. Sci. 12, 43.

Satyanarayana, D.N., 2001. Electronic Absorption Spectroscopy and Related Techniques. University Press, Hyderabad.

Sengupta, A., Clifford, K., Subramoniau, S., 1986. Chromate ion–exchange process at alkaline pH. Water Research 20 (9), 77–89.

Silversten, R.M., Webster, F.X., 1998. Spectroscopic Identification of Organic Compounds, 6th ed. Wiley, New York.

Tella, A.C., Owaludu, S.O., 2007. Some Langmuir and Freundlich parameters of studies of chloropheniramine maleate. Res. J. Appl. Sci. 2 (8), 875.

Vadi, M., Abbasi, M., Zakeri, M., Yazdi, B.J., 2010. Application of the Freundlich Langmuir Temkin and Harkins-Jura adsorption isotherms for some amino acids and amino acids complexation with manganese ion(II) on carbon nanotube. J. Phys. Theor. Chem. IAU Iran 7 (2), 95–104.

Zhu, Y., Millan, E., Sengupta, A.K., 1990. Separation of toxic metal cat ions by chelating polymers. React. Polym. 13, 241–253.